Optical conoscopy of distorted uniaxial liquid crystals: computer simulation and experiment.

Yu.A.Nastishin, O.B.Dovgyi, O.G.Vlokh

Institute for Physical Optics, 23 Dragomanov str., L'viv 290005, Ukraine

Received 05.06.2001

Abstract

We propose an algorithm to compute the conoscopic pattern for distorted uniaxial liquid crystal cells. The computed conoscopic figures for several cells (homeotropic, planar, twist, hybrid, hybrid under an external field) are compared to the corresponding experimental conoscopic patterns. We demonstrate that conoscopy can be used for the characterization of the distorted nematic cells with the director deformations which can not be detected and unambigously characterized by direct microscopy observations and other techniques.

Keywords: optical conoscopy, uniaxial single crystals, distorted liquid crystal, birefringence, computer simulation.

PACS: 42.25.Lc, 42.30.Sy, 42.70Df

1. Introduction

Optical conoscopy is one of the most often used optical techniques for the characterization of solid optical single crystals. The observation of the conoscopic figures precedes to any optical investigation of a newly grown (or obtained in some other way) crystalline specimen. The conoscopic figure of a thick (~ 5mm) solid crystal can be easily obtained on a screen simply by laser illumination of the crystal placed between crossed polarizers. As soon as the conoscopic figure is observed, then according to known methods several important structural characteristics can be determined, namely: type of the crystal (uni- or biaxial), orientation of the optical axis (axes), optical sign, presence and sign of gyrotropy [1-4]. Although there is no principal difference between the conoscopic figures of conventional solid crystals and liquid crystals (LC's), the conoscopy is used for the characterization of LC's not very often. First of all the main information on the structure of the LC sample can be obtained by direct observation of its texture under the polarization microscope. There are some technical (but not principal) difficulties in the conoscopy of LC's. Usually LC samples are thinner than few tens of microns. As a result because of limited aperture only the isogyres and few isokhromes can be observed on the screen. Only the isogyres usually are observed under the polarization microscope, while isokhromes are out of the microscope field. Nevertheless in some special cases, as for example when it is necessary to establish whether the LC is uniaxial or biaxial the conoscopy is used [5-11]. The experimental observation of the conoscopic figures of the nematic cell under external field was used long time ago for the demonstration of the field reorientation effect in nematics [12]. The conoscopic figure of a twisted cell was analized theoretically by Maugin [13], and later Cladis [14] has used the analysis of the conoscopic picture for the measurement of the nematic twist elastic constant. The computation of the conoscopic figures of homogeneous LC's and the analysis of the influence of the lens aberrations were performed in [15]. It is also

worth noticing that the crystal rotation technique (CRT) [16] for the measurement of the pretilt angle of the director in a nematic cell, based on the analysis of the angle dependence of the transmittance of the cell between crossed polarizers, is nothing else but the analysis of one-dimensional cros-section of the conoscopic pattern. The conoscopy in its conventional application is developed mostly for the characterization of single crystals. We did not find in literature the description of the conoscopic figures calculation for distorted liquid crystals. The aim of this paper is to represent a simple algorithm for the computation of the conoscopic figures for the continuously distorted uniaxial liquid crystals and to stress the advantages of the conoscopy for the characterization of the LC cells. As an example we refer to the situation when the pretilt angle values of the director on two substrates of a quasi homeotropic LC cell are slightly different. One says that the cell possesses hybridity. Polarization microscope observations as well as CRT [16] can not distinguish between the uniform nematic cell with tilted director and the cell in which director field is distorted in the plane perpendicular to the substrates. According to [17,18], hybridity can be detected at the measurements of the pretilt angle by so-called Magnetic Null Technique [19] with light probing at different angles of the light beam with respect to the LC cell. Here we demonstrate that the conoscopy visualizes the hybridity of a quasi homeotropic cell and characterizes it quantitatively.

In the next section we represent the algorithms to compute the conoscopic figures for several LC cells. The conoscopic patterns can be plotted using Mathematica or Maple packages.

2. Algorithms for computation of the conoscopical figures

A conoscopic figure displays a two-dimensional distribution of the intensity $I(x,y)$ of diverged light passed through the crystal, which is placed between the crossed polarizers. If the structure of the LC sample is known, the function $I(x,y)$ can be calculated numerically or analitically depending on the character of the space distribution of the optical axis in a given sample.

The conoscopic figure contains two types of lines: isokhromes and isogyres. The isokhromes are the lines of constant phase retardation. When the optical axis is normal to the sample surface (angle $\theta=0^o$) and parallel to the axis of the diverged light beam, the isokhrome equation is the equation of the family of circles [1-4]. If the optical axis is tilted ($0<\theta<\pi/2$) the exact equation for isokhromes is a quite complicated transcendental equation even for the uniform uniaxial single crystal. Using the approximation of small aperture one can simplify this equation to the equation of an ellipse or hyperbola for small and large θ respectively [2]. Usually in the books on crystalloptics (see for example [1-4]) the analysis of the conoscopic picture of an uniaxial single crystal is restricted to the analysis of the isokhrome equation. For uniaxial single crystals the shape of isogyres usually is considered to be trivial. Indeed, for uniaxial uniform single crystals the isogyres are parallel to the polarization directions of the polarizer and analyzer. They have a shape of Maltese cross centered in the exit point of the optical axis, defined by the angle θ. If the single crystal is uniform, the shape of the isogyres is not sensitive to the angle θ value. This is not the case of a distorted LC cell. The isogyres as well as isokhromes visualize the distortion of the director field.

2.1. Uniform distribution of the optical axis

Let us consider a nonabsorbing uniaxial liquid crystal between parallel transparent substrates which is placed between crossed polarizers. Let the Z-axis of the coordinate system be along the normal to the substrates and the X-axis be along the polarizer direction (Fig.1). We consider the

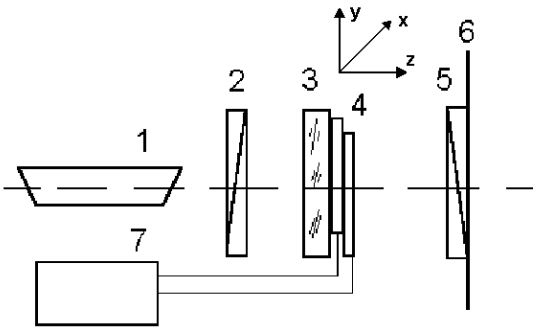

Fig.1. The Cartesian coordinate system and experimental set-up; 1 - laser, 2 - polariser, 3 - scattering plate, 4 - cell, 5 - analyzer, 6 - screen, 7 - power supply. The diverged geometry of the light beam is obtained by scattering on the unpolished glass plate (3).

polarizer and analyzer as ideal optical elements of negligible thickness and reflectance, with the polarization efficiency independent on the light incident angle, with their planes attached to the substrates. A monochromatic (λ=0.6 μm) light beam passing through the polarizer is focused in the origin of the coordinate system located on the first LC interface (Fig.2). The diverged beam with uniform in-plane intensity I_0 is symmetrical with respect to the *Z*-axis. The optical axis is uniformly distributed inside the sample and is defined by the polar angle θ and the azimuth angle γ.

Linearly polarized light ray, which is incident on the crystal plate at some angle to the *Z*-axis is divided at the crystal surface into reflected and transmitted components. In most practical cases the reflection is weak and does not modify essentially the conoscopic figures, but makes calculations quite complex. In our calculations we neglect the reflection and assume that the light energy is transferred without losses through the sample. The refracted ray propagates in a crystal as two eigen waves (also termed as normal waves): ordinary and extraordinary ones. In the first approximation the eigen waves are linearly polarized plane waves. The electrical vector of the ordinary wave vibrates in the direction C_o perpendicular to the so called principal plane containing the wave vector and optical axis. The electrical vector of the extraordinary wave is directed along the vector C_e located in the principal plane. The ordinary and extraordinary waves have different refractive indices and propagate along different directions according to the Snell's law. Exiting from the sample these eigen waves interfere. The amplitude of the resulting wave depends on the phase shift between interfering eigen waves. There are two contributions to the phase shift: the difference in the eigen waves refractive indices and the difference in the pass lengths for two rays. One can show that for small angle aperture the second contribution can be neglected comparing with the first one (see [1-4]). With a good approximation one can accept that the ordinary and extraordinary waves propagate along the

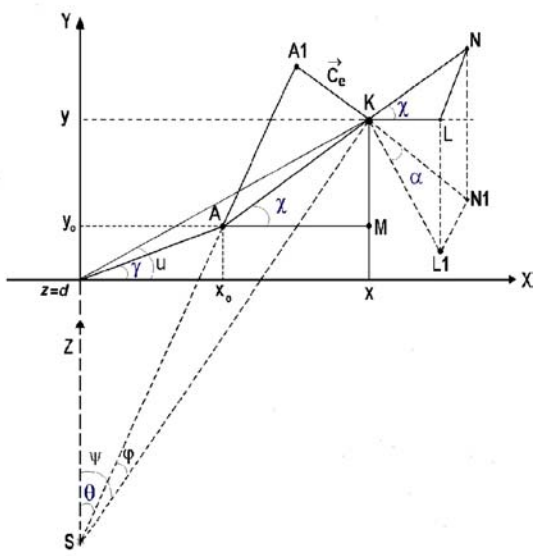

Fig.2. To the definition of the computation parameters. The semi plane *y>0, z=d* is in the plane of the page and is overlapped with the analyzer and screen planes. For the convenience the semi-plane *y=0, 0<z<d* is depicted in the plane of the page but keeping in mind that really this plane is perpendicular to the semi-plane *y>0, z=d. S* is the origin of the coordinate system. *A* and *K* are located in the plane *z=d* and are the exit points of the optical axis *SA* and of a given ray *SK* with the wave vector *k,* of the diverged light beam, respectively. *K(x,y)* is a given point of the conoscopic picture.

same geometrical path, but with different refractive indices. In this approximation the eigen wave vectors k_o and k_e are replaced by the wave vector k of a light ray propagating along the bisectrix between k_o and k_e. In Fig. 2 three vectors: C_e (along AK_1), vawe vector k (along SK) and the optical axis SA_1 create rectangular triangle with C_e and k being its cathetuses. The orientation of the ray can be described by the polar angle ψ and the azimuth angle u. The angle ψ can be calculated from the Snell's law in the assumption that the light ray propagates with the average refractive index.

The transmitted light waves passing through the analyzer display the interference pattern on the screen. The interference picture is of the form:

$$I(x,y) = I_0 \sin^2[\Delta(x,y)/2] \sin^2[2\alpha(x,y)], \quad (1)$$

where $\Delta(x,y)$ is the phase retardation:

$$\Delta = (2\pi/\lambda)\, n\, \Delta n\, \rho \sin^2\phi \quad (2)$$

Here for the simplification we use the approximation

$$\Delta n_{eff} = \Delta n \sin^2\phi \quad (2a)$$

Δn_{eff} is the birefringence for a given ray, $\Delta n = n_{//} - n_{\perp}$ is the difference between the refractive indices along and perpendicularly to the optical axis respectively, $n = (n_{//} + n_{\perp})/2$ is the average refractive index, ϕ is the angle KSA_1 between the ray direction and the optical axis, ρ is the radius-vector of a given point of the conoscopic pattern on the screen. For typical LC Δn values the approximation (2a) gives relative error smaller than 4% in comparisson with the exact expression

$$\Delta n_{eff} = n_0 - n_0 n_e / ((n_0 \sin(\phi))^2 + (n_e \cos(\phi))^2)^{1/2}.$$

From Fig.1 we have:

$$\cos\phi = \cos\psi \cos\theta + \sin\psi \sin\theta \cos(\gamma - u) \quad (3)$$

$$\rho = d\, tg\psi \quad (4)$$

In the Cartesian coordinates equations (3),(4) are

$$\cos\phi = \{d\cos\theta + \\ + \sin\theta (x\cos\gamma + y\sin\gamma)\} (x^2+y^2+d^2)^{-1/2} \quad (5)$$

$$\rho = (x^2+y^2+d^2)^{1/2} \quad (6)$$

In equation (1) the angle α is the angle between the principal plane and the polarization plane of the incident ray, i.e. the angle between the vector C_e and the polarization direction C_i of the incident ray. In the approximation of small ψ one can replace α by the angle χ, which is the angle between the projections of the vectors C_e and C_i on the screen plane. The approximation

$$\alpha(x,y) \approx \chi(x,y) \quad (7)$$

also implies that we do not take into account the phenomena of the change of the polarization at the interfaces due to reflection and scattering, including the angle dependence of the polarizers efficiency and depolarization on the scattering plate, which we use in our experiment to obtain a diverged beam. The deviation from the approximation (7) will contribute to a real conoscopic pattern decreasing its contrast but not affecting essentially the shape of the isochromes and isogyres.

From Fig.2 we express χ as the function of the x,y coordinates :

$$\sin 2\chi = 2(x\cos\theta - d\sin\theta\cos\gamma) \\ (y\cos\theta - d\sin\theta\sin\gamma) / [(x\cos\theta - \\ d\sin\theta\cos\gamma)^2 + (y\cos\theta - d\sin\theta\sin\gamma)^2] \quad (8)$$

The system of equations (1), (2), (5), (6), (8) is the algorithm for the computation of the conocsopic pattern of an uniaxial crystal with tilted optical axis. Fig.3 shows the Density Plots for the homeotropic *(a)*, tilted (c, $\theta=10^o$; d, $\theta=85^o$) and planar *(e)* orientations of the optical axis calculated for d=25μm, Δn=0.18, n=1.5, λ=0.6μm; and corresponding experimental conoscopic patterns (Fig. 3 *b, f*). The plotted conoscopic figures (Fig.3 *a, c, d, e*) visualize the principle of the Crystal Rotation Technique: light intensity distribution is symmetrical with respect to the exit point of the optical axis (in terms of Crystal Rotation Technique with respect to the angle θ).

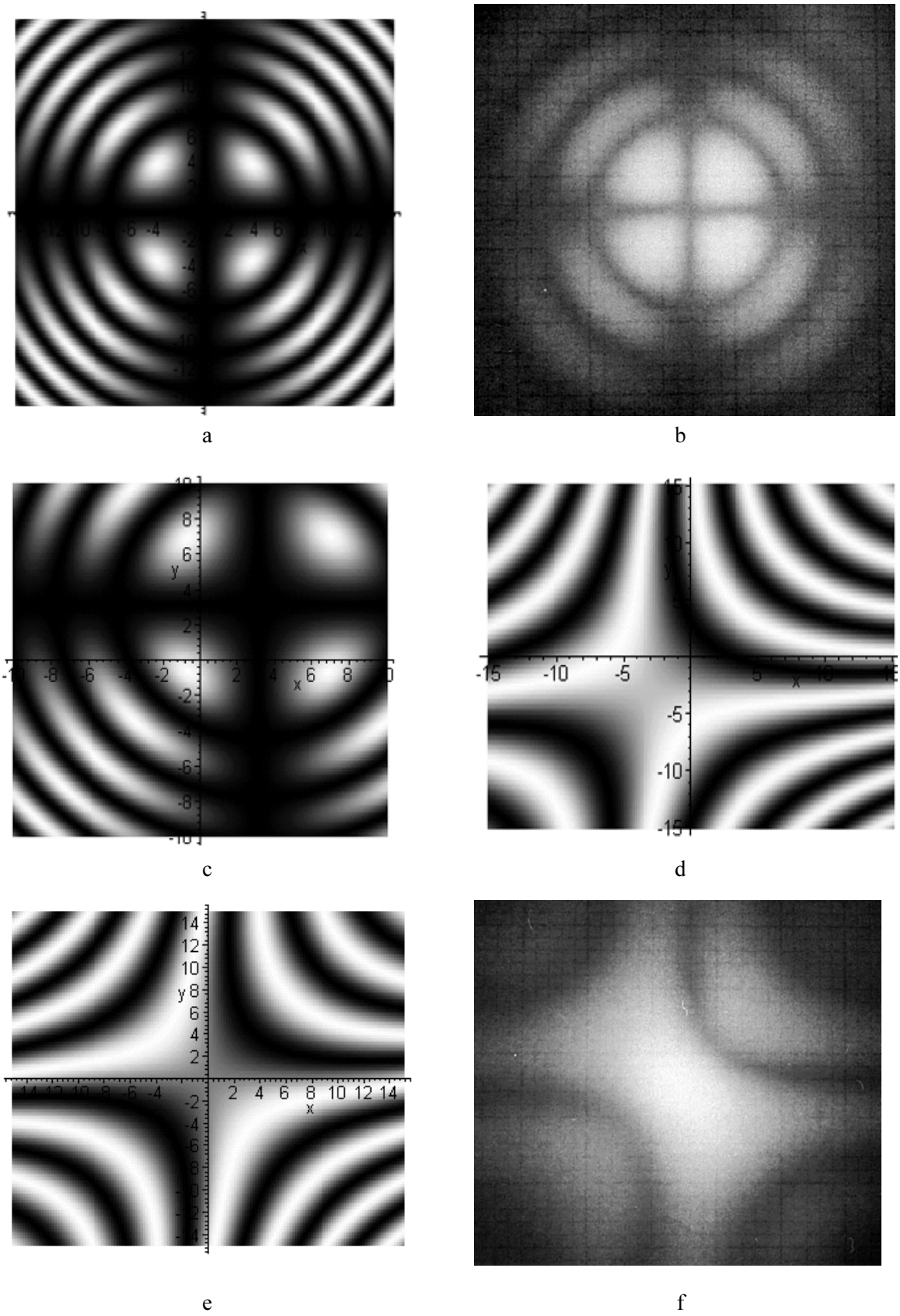

Fig.3. Computed (*a*, *c, d, e*) and experimental conoscopic patterns (*b, f*) for different uniform director orientations with $\gamma_0=\gamma_d=45^o$: homeotropic, $\theta=0^o$ - *a,b*; tilted, $\theta=10^o$ – *c*, $\theta=85^o$ – *d;* planar, $\theta=90^o$ – *e, f*.

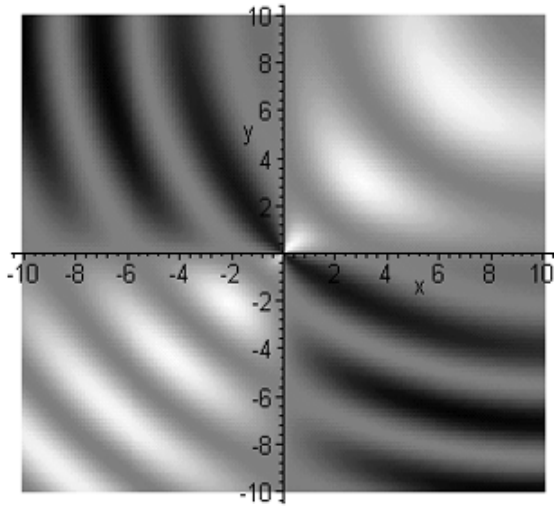

a

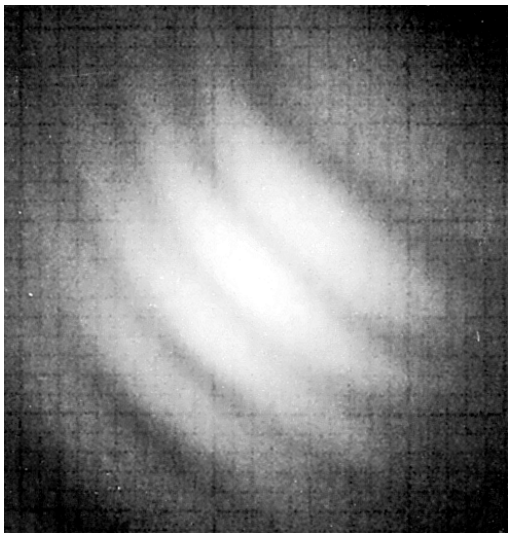

b

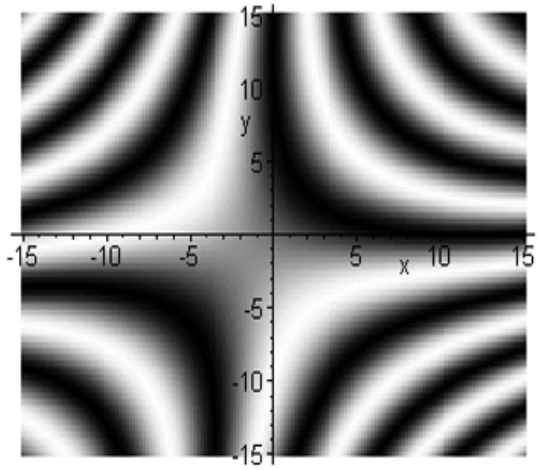

c

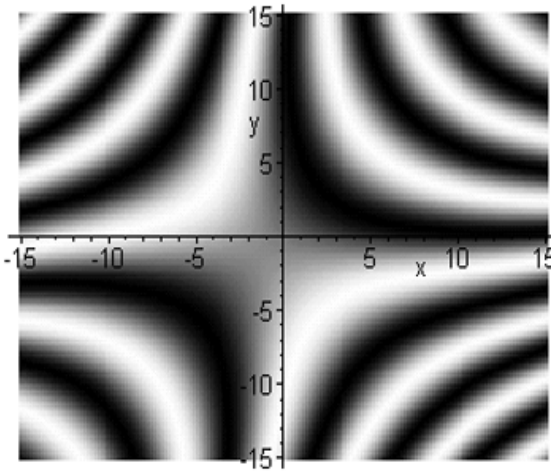

d

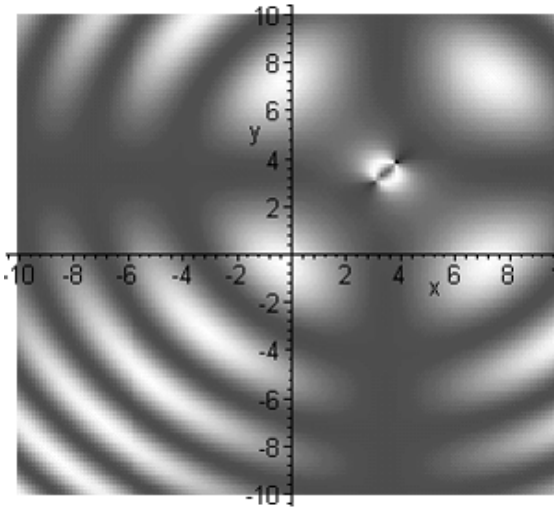

e

Fig.4. Computed (a, c, d, e) and experimental conoscopic patterns (b) for the cells with hybridity; $\gamma_0=\gamma_d=45^\circ$: a,b) $\theta_0=0^\circ$, $\theta_d=90^0$; c) $\theta_0=85^\circ$, $\theta_d=90^0$; d) $\theta_0=\theta_d=87.5^0$; e) $\theta_0=10^\circ$, $\theta_d=12^0$.

2.2. Twisted hybrid cell

The twisted hybrid cell is the nematic cell with the following surface conditions

$$\theta(z=0) = \theta_0,\ \theta(z=d) = \theta_d \quad (9a)$$

$$\gamma(z=0) = \gamma_0,\ \gamma(z=d) = \gamma_d \quad (9b)$$

The z-profile of the optical axis is

$$\theta = \theta_0 + (z/d)\,(\theta_d - \theta_0) \quad (10a)$$

$$\gamma = \gamma_0 + (z/d)\,(\gamma_d - \gamma_0) \quad (10b)$$

Light intensity passed through the cell and analyzer is of the form:

$$I = I_0\{\sin^2(\chi_d - \chi_0) + \sin^2(\Delta_a/2)\sin 2\chi_0 \sin 2\chi_d\}, \quad (11)$$

where

$$\Delta_a = (\pi/\lambda) n\,\Delta n\,\rho[1+\sin^2\psi\sin^2(u-\gamma_0) - (\sin[\Delta\theta]/\Delta\theta)\times\{\cos(2\phi_a) + \sin^2\psi\sin^2(u-\gamma_0)\}] \quad (12)$$

is the phase retardation obtained by integrating (2) on conditions (9a,10a), $\Delta\theta = \theta_d - \theta_0$,

$$\cos\phi_a = \cos\psi\cos\theta_a + \sin\psi\sin\theta_a\cos(u-\gamma_0) \quad (13)$$

$$\theta_a = (\theta_d + \theta_0)/2;$$
$$\cos u = x/(x^2+y^2)^{1/2};$$
$$\sin u = y/(x^2+y^2)^{1/2}; \quad (14)$$
$$\cos\psi = d/(x^2+y^2+d^2)^{1/2};$$
$$\sin\psi = (x^2+y^2)^{1/2}/(x^2+y^2+d^2)^{1/2}.$$

$\rho = (x^2+y^2+d^2)^{1/2}$ is the radius-vector of a given point of the conoscopic pattern, $\theta_a = (\theta_d + \theta_0)/2$,

$$\sin 2\chi_{0,d} = 2(x\cos\theta_{0,d} - d\sin\theta_{0,d}\cos\gamma_{0,d})\,(y\cos\theta_{0,d} - d\sin\theta_{0,d}\sin\gamma)\,/\,[(x\cos\theta_{0,d} - d\sin\theta_{0,d}\cos\gamma_{0,d})^2 + (y\cos\theta_{0,d} - d\sin\theta_{0,d}\sin\gamma_{0,d})^2] \quad (15)$$

The system of equations (11-15) is the algorithm for the computation of the conoscopic pattern of a twisted hybrid cell. At $\gamma_0 = \gamma_d$ these equations describe a hybrid cell. The calculated and experimental conoscopic pattern of the hybrid cell with $\theta_0 = 0^o$, $\theta_d = 90^o$, $\gamma_0 = \gamma_d = 45^o$ for d=25μm, Δn=0.18, n=1.5, λ=0.6μm are shown in Fig. 4*a,b*. In principle, equation (11) can be applied to any continuously distorted nematic cell. If the distribution of the director is known, the phase retardation can be calculated analytically or numerically and substituted into (11). The equation for the isochromes is:

$$\sin^2[\Delta_a/2] = 0 \quad (16)$$

The term $\sin^2[\chi_d - \chi_0]$ in (11) decreases the contrast of the conoscopic pattern. Two equations: $\chi_0 = 0$, $\chi_d = 0$ describe the isogyres. When $\theta_0 \neq \theta_d$ the isogyres pair off into two sets of two brushes intersected in the points with coordinates $x_{0,d} = d\,tg\theta_{0,d}\cos\gamma_{0,d}$, $y_{0,d} = d\,tg\theta_{0,d}\sin\gamma_{0,d}$ respectivelly (Fig.4 *e*). The distance between these points on the screen is proportional to the difference $tg\theta_d - tg\theta_0$. These features can be used for the characterization of quasi-homeotropic cell as a test for hybridity. The phase retardation of a hybrid cell does not depend on θ_0 or θ_d but is a function of the average angle $\theta_a = (\theta_0 + \theta_d)/2$, while the location of the isogyres depends on θ_0 and θ_d. When the isogyres are observed the hybridity is visualized. For a quasi-planar cell ($\theta_{0,d} \approx \pi/2$, $x_{0,d} \to \infty$, $y_{0,d} \to \infty$) the isogyres are not seen. As a result the hybridity of the quasi-planar cell is not displayed on the conoscopic pattern. From Fig. 4 *c, d* it is seen that the simulated conoscopic pattern of the cell with $\theta_0 = \theta_d = 87.5^o$ (Fig. 4 d) is equivalent to the picture of the cell with $\theta_0 = 85^o$, $\theta_d = 90^0$ (i.e with the average angle $\theta_a = 87.5^o$ (Fig. 4 *c*)). The light intensity distribution is symmetrical with respect to the point (x_0, y_0) corresponding to the angle $\theta_a = 87.5^o$.

2.3. Hybrid cell under transverse field

In most practical cases the orientation of the director in a nematic cell under an external field (magnetic or electric) is a non-analitical function of the distance from the limitting surfaces and is defined by the competition of the orienting action of the field and of the substrates. The director distribution can be obtained by the free energy minimization. The exact solution of the Euler-Lagrange equation implies numerical calculations. At these calculations it is usually assumed

that the director distribution is a two dimensional one. At high fields in the middle of the cell and far from the substrates the director is oriented practically along ($\Delta\varepsilon>0$) the field direction. In the hybrid cell under transverse electric field the director deformation is located in a thin layer near the substrate with planar surface conditions. The polar angle θ_0 of the director on the surface as well as the thickness of the layer containing the deformation decrease when the field strength increases. The optical properties of hybrid cell of thickness d under the field can be modeled by a pile of two nematic layers, namely: a homeotropic layer of thickness h and a hybrid one with the limitting polar angles θ_0, $\pi/2$ of the thickness d-h. The phase retardation of the cell is:

$$\Delta_H=(2\pi/\lambda)(n\Delta n/\cos\psi)\left[h\sin^2\psi+(d-h)\{1-(1/2)*\right.$$

$$\left.[C_+ -(\sin\Delta\theta/\Delta\theta)(b\sin 2\theta_a + C_- \cos(2\theta_a)]\}\right] \quad (17)$$

where

$$C_+ = \cos^2\psi + \sin^2\psi\cos^2(u-\gamma_0);$$

$$C_- = \cos^2\psi - \sin^2\psi\cos^2(u-\gamma_0);$$

$$b = \sin 2\psi\cos(u-\gamma_0).$$

$\sin\psi$ and $\cos\psi$ are given by equations (14). Here $\Delta\theta = \theta_0$, $\theta_a=\theta_0/2$. The azimuths χ_0 and χ_d can be calculated from Eq. (15). The procedure of the change of θ_0 and h models the variation of the field strength. Collating θ_0 and h we obtained computer simulated conoscopic figures simillar to the experimental pictures (see for example Fig. 5*a* and 5*b*).

We applied electric field to the hybrid nematic (dielectric anizotropy $\Delta\varepsilon>0$) cell and observed the transformations of the conoscopic pattern. We show three experimental conoscopic patterns of the hybrid cell at zero (Fig.4*b*); intermediate, (Fig.5*b*); and high, (Fig.5*c*) voltages. In this paper we represent the computed figures only as an illustration of the validity of the algorithms without detailed discussion of the experimental and simulated figures. This study is subject of our forthcoming paper.

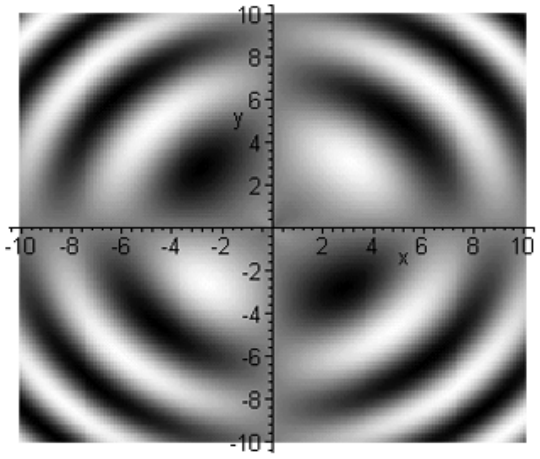

a

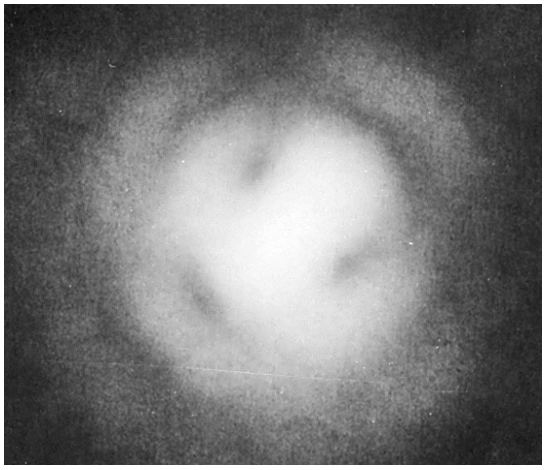

b

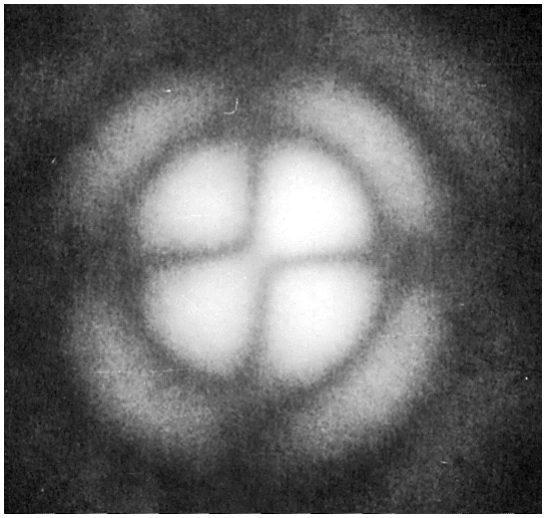

c

Fig.5. Computed (*a*, θ_0=89°, θ_d=0°, h=24μm, d=25μm) and experimental (*b*, 8V and *c*, 48V) conoscopic patterns for the hybrid cell under electric field (f=100 kHz).

3. Conclusion

We proposed the algorithm for computer simulations of the conoscopic patterns of the distorted nematic cells. The validity of the algorithm is demonstrated by the comparisson of the computed and corresponding experimental conoscopic patterns. The conoscopy can be used as a test for hybridity in a quasi homeotropic cell, and for twist in any continuously distorted nematic cell even when the distortion cannot be characterized by conventional polarization microscopy.

Acknowledgements. We are grateful to M.Kleman, S.Asnasios, C.Meyer for helpful discussion and to M. Kostyrko and L.Pelykh for their assistance. The Laboratoire de Mineralogie Crystallographie de Paris, Universite P. et M. Curie is acknowledged for the hospitality for one of us (Yu.N.) during the stay in this laboratory and for the possibility to use their Mathematica package.

References

1. Born M. and Wolf E. Principles of Optics. Pergamon Press, 4th ed., (1970).
2. Konstantinova A.F., Grechushnikov B.N., Bokut B.V., Valyashko E.G. Optical properties of crystals. Minsk. "Navuka i Technika", (1995). (in Russian)
3. Vlokh O.G. Phenomena of space dispersion in parametric crystalloptics. Lviv. "Vyshcha shkola", (1984). (in Russian)
4. Romanyuk M.O. Crystalloptics. Kiev. IZMN. (1997). (in Ukrainian)
5. Yu L.J.and Saupe A., Phys. Rev. Lett. **45**, (1980) 1000.
6. Chandrasekhar S., Nair Geetha G., Rao D. S. Shankar, Prasad S. Krishna, Praefcke K., Blunk D. Curr.Sci. **75** (1998) 1042-1046.
7. Galerne Y. and Marcerou J.P. Phys. Rev. Lett., **51**, **23**,(1983)2109.
8. Gorechka E., Chandani A.D.L., Ouchi Yu., Takezoe H., Fukuda A. Jpn. J. Appl.Phys., **29**,**1**,(1990) 131.
9. Moritake H., Ozaki M., Tanigushi H., Satoh K., Yoshino K. Jpn. J. Appl.Phys., **33**, Part 1,No.9B, (1994)5503.
10. Fujikava T., Hiraoka K., Isoaki T., Kajikava K., Takezoe H., Fukuda A.. Jpn. J. Appl.Phys., **32**, Part 1, No.2, (1993)985.
11. Natano J., Nanaki Y., Furue H., Uehara H., Saito Sh., Murashiro K. Jpn. J. Appl.Phys., 33, Part 1, No.9B, (1994)5498.
12. Prost, J. and Gasparoux, H. C. R. Acad. Sci., Paris C273(1972) 335.
13. Maughin, Bull C. Soc. fr. Miner. **34**, (1911) 71.
14. Cladis P.E.. Phys. Rev. Lett. 31,(1973)1200.
15. MacGregor A.R.. J. Opt. Soc. Am. A, vol.7, No.3,(1999)337.
16. Baur G., Wittwer V. and Berreman D.W. Phys. Lett. A **56**, (1972)142.
17. Andrienko D., Kurioz Y., Reznikov Y., Rozenblatt C., Petchek R., Lavrentovich O.and Subacius D. J.Appl.Phys. **83**, (1998)50.
18. Ziherl P., Subacius D., Strigazzi A., Pergamenshchik V.M., Alexe-Ionesku A.L., Lavrentovich O.D. and Zumer S. Liq. Cryst. **24**, (1998)607.
19. Sheffer T.J.and Nehring J. J.Appl. Phys. **48**, (1977) 1873.